# FERMILAB BOOSTER BEAM EMITTANCES FROM QUADRUPOLE MODES MEASURED BY BPMs*

C. Y. Tan†, M. Balcewicz, Fermi National Accelerator Laboratory, Batavia, IL60510, USA

*Abstract*

The measurement of beam emittances by extracting the quadrupole mode signal from a 4 plate beam position monitor (BPM) was published at least 40 years ago. Unfortunately, in practice, this method suffers from poor signal to noise ratio and requires a lot of tuning to extract out the emittances. In this paper, an improved method where multiple BPMs are used together with better mathematical analysis is described. The BPM derived emittances are then compared with those measured by the Ion Profile Monitor (IPM). Surprisingly, the BPM measured emittances behave very well and are more realistic than those measured by the IPM.

## INTRODUCTION

The measurement of beam emittances by extracting the quadrupole mode signal from a 4 plate beam position monitors (BPM) was published at least 40 years ago [1, 2]. However, the quadrupole signal is very small when compared to the dipole signal and so, in practice, this method suffers from poor signal to noise [3]. This means that to actually get the emittance, a lot of tuning is required. We decided a revisit of this method because the Booster Ionization Profile Monitors (IPMs) have idiosyncrasies that are very puzzling [4]. For example, the beam current measured by the IPM is not conserved. It also shows an emittance growth during the Booster ramp that is unexplained [5].

Our contribution to the improvement of this method are the use of multiple BPMs which then gives us a better way for emittance extraction. When we compared the emittances extracted with our method to those measured by the IPMs in the Booster, we found that the BPM measured emittances were more realistic than those from the IPMs.

## THEORY

This section only contains an abridged version of the theory. A full derivation can be found in Ref. [6] which follows Miller [1].

The cross section of the 4 plate BPM is shown in Fig. 1. The image current density, $J_w$, that is induced by a pencil current, $I_b$, at $(r_b, \theta_b)$ is given by

$$J_w(r_b,\theta_b;b,\phi_w) = -\frac{I_b(r_b,\theta_b)}{2\pi a}\left[1+2\sum_{n=1}^{\infty}\left(\frac{r_b}{a}\right)^n \cos n\left(\phi_w-\theta_b\right)\right]. \quad (1)$$

We can integrate the above to obtain the current on each plate $R$(ight), $L$(eft), $T$(op) and $B$(ottom). For example the current on the $R$(ight) plate, $I_R$, is simply $I_R = \int_{-\phi_0/2}^{\phi_0/2} d\phi\ aJ_w$ to give

$$I_R = -\frac{I_b(x_b,y_b)}{2\pi}\left\{\phi_0+2\left[2\left(\frac{x_b}{a}\right)\sin\frac{\phi_0}{2}+\left(\frac{x_b^2-y_b^2}{a^2}\right)\sin\phi_0\right]\right\}. \quad (2)$$

where we have only kept terms lower than $(r_b/a)^3$. We can obtain similar equations for $I_L$, $I_T$ and $I_B$.

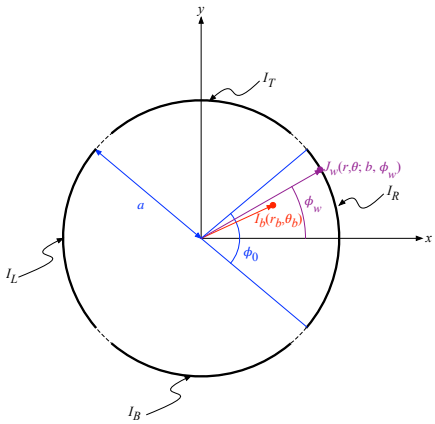


Figure 1: This cartoon shows the line current $I_b$ at $(r_b, \theta_b)$ inducing a current density on the $R$(ight) pickup plate. All the plates have radius $a$ and subtends an angle $\phi_0$. The current density at $(a, \phi_w)$ is $J_w$.

And if the transverse distribution of the beam is a bi-gaussian distribution centred at $(\bar{x}, \bar{y})$ with standard deviations $\sigma_x$ and $\sigma_y$ in the $x$ and $y$ directions respectively, then the normalized gaussian distribution function is

$$\rho(x,y) = \frac{1}{2\pi\sigma_x\sigma_y}\exp\left[-\frac{(x-\bar{x})^2}{2\sigma_x^2}\right]\exp\left[-\frac{(y-\bar{y})^2}{2\sigma_y^2}\right]. \quad (3)$$

With the above density function, the new current distribution on the $R$(ight) plate is

$$R = \int_{-\infty}^{\infty} dx\ dy\ \rho I_R, = -\frac{I_b}{2\pi}\left\{\phi_0+2\left[2\left(\frac{\bar{x}}{a}\right)\sin\frac{\phi_0}{2}+\left(\frac{\sigma_x^2-\sigma_y^2}{a^2}+\frac{\bar{x}^2-\bar{y}^2}{a^2}\right)\sin\phi_0\right]\right\}. \quad (4)$$

The remaining plates will also have a similar current distributions $L$, $T$, $B$.

Finally, we can take the appropriate sum and difference combinations of $R$, $L$, $T$ and $B$ to create the dipole modes,

* This manuscript has been authored by Fermi Research Alliance, LLC under Contract No. DE-AC02-07CH11359 with the U.S. Department of Energy, Office of Science, Office of High Energy Physics.

† cytan@fnal.gov

$d_x$ and $d_y$ and quadrupole mode $q$

$$\left.\begin{aligned} d_x &= \frac{R-L}{R+L+T+B} = \frac{\sin\frac{\phi_0}{2}}{\frac{\phi_0}{2}}\left(\frac{\bar{x}}{a}\right) \\ d_y &= \frac{T-B}{R+L+T+B} = \frac{\sin\frac{\phi_0}{2}}{\frac{\phi_0}{2}}\left(\frac{\bar{y}}{a}\right) \\ q &= \frac{2\sin\phi_0}{\phi_0}\left(\frac{\sigma_x^2-\sigma_y^2}{a^2}+\frac{\bar{x}^2-\bar{y}^2}{a^2}\right) \end{aligned}\right\}. \quad (5)$$

$q$ can be written in terms of $d_x$ and $d_y$ to give

$$q-(d_x^2-d_y^2)\phi_0\cot\frac{\phi_0}{2} = \frac{2\sin\phi_0}{\phi_0}\left(\frac{\sigma_x^2-\sigma_y^2}{a^2}\right). \quad (6)$$

The above can be written In terms of lattice functions by using the following relationship

$$\sigma_{x,y}^2 = \frac{\beta_{x,y}\epsilon_{x,y}}{\pi}+(D_{x,y}\sigma_p)^2 \quad (7)$$

where $\epsilon_{x,y}$ are the emittances, $\beta_{x,y}$ are the beta functions, $D_{x,y}$ are the dispersions of the beam in the $x$ and $y$ directions respectively; and $\sigma_p^2 = \langle(dp/p)^2\rangle$ is the standard deviation of the relative momentum spread of the beam.

Thus, Eq. (6) becomes

$$\Delta_q \equiv \frac{2}{a^2}\frac{\sin\phi_0}{\phi_0}\left[\frac{\beta_x\epsilon_x}{\pi}-\frac{\beta_y\epsilon_y}{\pi}+(D_x\sigma_p)^2\right] \quad (8)$$

where $\Delta_q$ is as defined above and we have set $D_y = 0$ because the vertical dispersion is small in Booster.

We can write down a matrix equation using the above from the measurements of 1 to $n$ BPMs or 1 to $n$ samples from $m$ BPMs

$$\begin{pmatrix} \beta_x(1) & -\beta_y(1) & D_x^2(1) \\ \beta_x(2) & -\beta_y(2) & D_x^2(2) \\ \vdots & \vdots & \vdots \\ \beta_x(j) & -\beta_y(j) & D_x^2(j) \\ \vdots & \vdots & \vdots \\ \beta_x(n) & -\beta_y(n) & D_x^2(n) \end{pmatrix}\begin{pmatrix} \epsilon_x/\pi \\ \epsilon_y/\pi \\ \sigma_p^2 \end{pmatrix} = \frac{a^2\phi_0}{2\sin\phi_0}\begin{pmatrix} \Delta_q(1) \\ \Delta_q(2) \\ \vdots \\ \Delta_q(j) \\ \vdots \\ \Delta_q(n) \end{pmatrix} \quad (9)$$

where the $j$th row comes from the $j$th pickup or the $j$th sample. If $n > 3$ then we have a non-square matrix on the lhs, which means that we have an over-determined set of equations. This non-square matrix is easily inverted using SVD methods. See for example, *Mathematica*'s `PseudoInverse[]` function.

## *Data Manipulations*

If we naïvely perform the inversion in Eq. (9) to obtain the emittances, we will find that we will get garbage. The keys for getting sensible emittances are discussed below.

1. Theoretically, the gain on each BPM plate is required to be the same for Eq. (9) to work. Therefore, we have to correct the signal from the BPM plates to ensure that this condition is satisfied. Note: The choice of gain is critical for ensuring the emittance solutions are real and not complex. Details about our method is discussed in Ref. [6].

2. Any DC offsets from each BPM plate when there is no beam.

3. The most important observation of Eq. (9) is that on the rhs, there is the difference $\beta_x\epsilon_x/\pi - \beta_y\epsilon_y/\pi$. This means that if we had a round beam and $\beta_x \approx \beta_y$ then this difference is close to zero. So, in this configuration, it may not be possible to actually extract out the emittances. The ideal situation for extracting out the emittances would be to have one of the $\beta$'s be a lot larger than the other, i.e. either $\beta_x \gg \beta_y$ or $\beta_x \ll \beta_y$.

For the Booster, the BPMs in the S locations are good for extracting $\epsilon_x$ because $\beta_x(30\,\text{m}) \gg \beta_y(5\,\text{m})$ while the BPMs at the L locations are good for extracting $\epsilon_y$ because $\beta_x(7\,\text{m}) \ll \beta_y(20\,\text{m})$.[1] Therefore, Eq. (9) must contain data from both L and S BPMs to get good $\epsilon_{x,y}$ solutions. In this paper, we have paired the data from S01 and L01, S02 and L02, etc. for solving Eq. (9).

## *Systematic Error Removal*

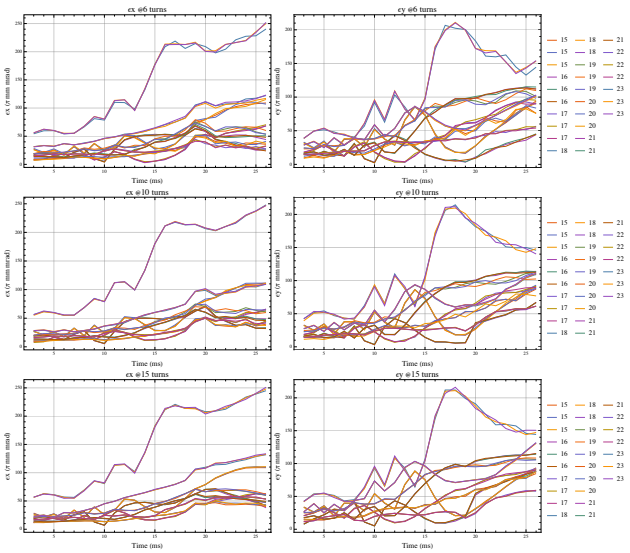


Figure 2: The systematic error of the emittances calculated with Eq. (9) for BPM pairs (L15, S15) to (L23, S23).

We will find that even after applying the keys in the previous section, the emittances found from Eq. (9) for every BPM pair have different, but reproducible, systematic errors. The systematic errors of each BPM pair (L15, S15) to (L23, S23) at three different beam intensities at 6, 10 and 15 turns[2] can be seen in Fig. 2. For each BPM pair, we have

[1] We are using the symbols "$\gg$" and "$\ll$" loosely here.

[2] The Linac beam is "stacked" in Booster in units of turns. Higher turns means higher intensity in Booster.

collected data at each intensity thrice to show that the curves are reproducible.

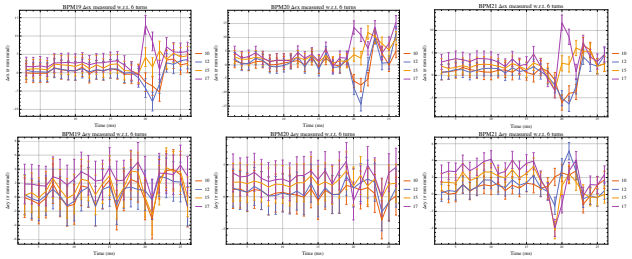

Figure 3: The horizontal and vertical emittance growth w.r.t. 6 turns for BPM pairs (L19, S19) to (L21, S21) for 10, 12, 15 and 17 turns are shown here.

Since the systematic error for each BPM pair is reproducible, we can simply correct it by defining the 6 turn curve in Fig. 2 to be the reference. We can then take the difference between any $n$ turn curve with the 6 turn curve to obtain the emittance growth w.r.t. 6 turns emittance. A sample of the horizontal and vertical emittance growth w.r.t. 6 turns for BPM pairs (L19, S19) to (L21, S21) for 10, 12, 15 and 17 turns are shown in Fig. 3.

From this example, although the curves from each BPM pair are not the same, we can identify some common features. This leads us to make the hypothesis that the differences are due to underlying random noise that can be averaged out *if* our system is ergodic. This means that we can average over the emittance from all the BPM pairs (space average) which should be the same as the averaged emittance at each BPM pair (time average).

## COMPARISON TO IPM EMITTANCE

The application of the ergodic hypothesis was the last step in the analysis of our method. At this point, we have to do some verification. One way to do this is to compare the BPM and IPM emittance measurements at different beam intensities.

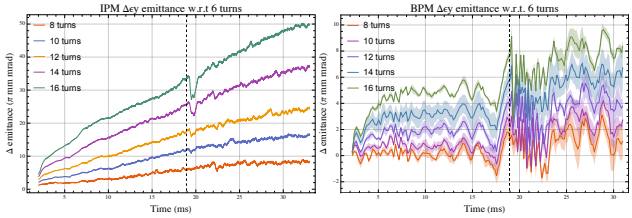


Figure 4: The vertical emittance growth w.r.t. 6 turns measured by the IPM (left) and the BPMs (right) for 8, 10, 12, 14, and 16 turns. The dotted line is where the beam crosses transition. Note: the IPM measured emittance is too large; the shaded regions in the right plot are the statistical 1 sigma spread of the emittance at each intensity. Sectors 5, 14 and 22 were ignored because of bad BPM data.

For the first test, shown in Fig. 4, we will look at the vertical emittance at different intensities because the vertical IPM is the reliable channel. Unfortunately, when we took the data, the IPM emittance results are at least a factor of 4 – 10 times too large and a linear growth which gets more steep as the intensity increases. We have not found any mechanism, including ecloud, that can cause this type of growth. On the other hand, the BPM emittance growth is a lot more realistic. The beam has an initial growth then flattens. A second growth happens after transition.

For the second test, we will look at the horizontal emittance. On a particular occasion (11 Jul 2023), the horizontal IPM functioned and returned data that looked reasonable *except* that it is too big by at least a factor of 4. Due to the lack of horizontal IPM data, we can only compare the IPM emittance growth taken on 11 Jul 2023 to the the BPM emittance growth data taken on 25 Mar 2024 in Fig. 5. Even though the data was taken about 7 months apart, they look similar, with the emittance oscillating after transition.

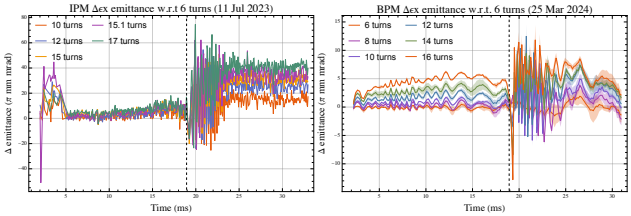


Figure 5: The horizontal emittance growth w.r.t. 6 turns measured by the IPM (left) and the BPMs (right) are shown here. The IPM emittance is about 4 times too large. Unfortunately, we can only compare data taken on different dates.

## CONCLUSION

We have improved the extraction of emittance from the BPM quadrupole mode by using multiple BPMs and with better data analysis. The compromise is that we do not measure absolute emittance but the emittance growth w.r.t. some reference. We have found that the emittance growth extracted from the BPM quadrupole mode looks more sensible than those measured by the IPMs. As part of making this method easy to use and without any expert tuning, we have written a python GUI to interact with the user and a `C++` program backend that can calculate Booster's emittance from real time BPM data. If this method proves to be as robust as we believe it to be, it opens up the ability of measuring emittances in nearly all rings that have 4 plate BPMs.

## ACKNOWLEDGMENTS

We would like to thank S. Chaurize, K. Triplett and J. Kuharik of the PS/Booster group who helped us take data. J. Diamond of the Controls group, R. Santucci and D. Steincamp of the Instrumentation group who helped us access the BPM frontends. V. Kapin of PS/Physics and R. Thurman-Keup of Instrumentation who helped us get the raw IPM data.

# REFERENCES


[1] R. H. Miller *et al.*, "Nonintercepting emittance monitor", SLAC, USA, Rep. SLAC-PUB-3186, Aug. 1983.

[2] G. Nassibian, "The measurement of the multipole coefficients of a cylindrical charge distribution", CERN, Geneva, Switzerland, Rep. CERN-SI-Note-EL-70-13, Dec. 1970.

[3] S. J. Russell and B. E. Carlsten, "Measuring emittance using beam position monitors", in *Proc. 15th IEEE Part. Accel. Conf.*, Washington, DC, USA, May 1993, pp. 2537–2539. doi:10.1109/PAC.1993.309381

[4] C. Bhat, "Booster IPM puzzle", https://beamdocs.fnal.gov/cgi-bin/sso/ShowDocument?docid=9264.

[5] V. Shiltsev, "On Booster intensity and IPM diagnostics (analysis of the 2019 Booster beam study S09 data)", https://beamdocs.fnal.gov/cgi-bin/sso/ShowDocument?docid=7997.

[6] C. Y. Tan, "Booster beam emittances from quadrupole modes measured by BPMs", https://beamdocs.fnal.gov/cgi-bin/sso/ShowDocument?docid=9916.